

# Fractional Horsepower Dynamometer - A General Purpose Hardware-In-The-Loop Real-Time Simulation Platform for Nonlinear Control Research and Education

Yashodhan Tarte<sup>†</sup>, *Student Member, IEEE*, YangQuan Chen<sup>†</sup>, *Senior Member, IEEE*, Wei Ren<sup>†</sup>, *Member, IEEE*  
and Kevin Moore<sup>††</sup>, *Senior Member, IEEE*

<sup>†</sup>Center for Self-Organizing and Intelligent Systems (CSOIS)  
Dept. of Electrical and Computer Engineering, 4160 Old Main Hill  
Utah State University, Logan, UT 84322-4160, USA

<sup>††</sup>Division of Engineering, Colorado School of Mines  
Golden, Colorado 80401-1887, USA

**Abstract**— A fractional horsepower dynamometer was developed as a general purpose hardware-in-the-loop real-time simulation platform to emulate mechanical nonlinearities such as frictions, state-dependent disturbances, etc. This lab system can be used as a research platform to test various nonlinear control schemes. This platform can also be used as a laboratory experiment for ECE5320 “*Mechatronics*” and ECE7330 “*Nonlinear and Adaptive Control*” courses at Utah State University. The novelty of this platform lies in its ability to generate an arbitrary external torque load disturbance, using a controllable hysteresis brake, to a DC motor plant. Therefore, many nonlinear systems and controls can be emulated physically. In this paper, we include some sample experimental results to show the versatility of the dynamometer in emulating nonlinearities and the effectiveness in real-time testing of advanced nonlinear control schemes.

**Index Terms**— Nonlinear control, adaptive control, hardware-in-the-loop real-time simulation, real-time control systems rapid prototyping

## I. INTRODUCTION

Topics like adaptive disturbance rejection in general and friction compensation in particular have been of special interest to control theorists, due to a wide variety of applications in the fields of robotics, automobiles, microelectromechanical systems etc. Advances in nonlinear control theory have made possible significant developments in these and other areas [1], [2]. It is widely accepted that the development of any new theory requires experimental supporting evidence. However, performing actual experiments on real world machines can be expensive. This gives rise to the need for a generic low-cost platform that can generate nonidealities like friction and other forms of disturbances.

The Center for Self-Organizing and Intelligent Systems (CSOIS) at Utah State University (USU) has developed a fractional horsepower dynamometer [3], shown in Fig. 1, equipped with DC motor, hysteresis brake, encoder for position feedback, load-cell for force feedback, and power and drive circuitry. The hysteresis brake is used to generate a brake force that acts as a disturbance to the motion of the motor shaft. As is proposed in this paper, this setup can be used to simulate various nonlinear control problems. Five example nonlinear adaptive control problems, namely, adaptive feedforward cancelation (AFC) [4], repetitive control (RC) [5], adaptive Coulomb friction compensation (ACFC) [6], state-periodic adaptive learning control (SPALC) [7] for state-periodic disturbance, and sliding mode control [8] are presented here with experimental results on this platform.

The Department of Electrical and Computer Engineering (ECE) at USU offers a graduate level course in Nonlinear and Adaptive

Control [9]. This course deals with nonlinear systems theory, stability analysis, and nonlinear feedback control design techniques. The department also offers a course in Mechatronics [10], which deals with principles, interfacing, and signal conditioning of motion sensors and actuator, the modeling, analysis, and identification of discrete-time systems, and digital controller design methods.

This paper describes how the fractional horsepower dynamometer can be used as a low-cost, real-time rapid prototyping platform to test nonlinear control algorithms as well as a laboratory experiment for the above mentioned courses. Section II describes the overall structure, including hardware and software, of the dynamometer. Section III provides the details of the proposed application of the dynamometer. Section IV gives the experimental results in support of the proposition. Finally, Section V draws conclusions from the results and outlines future possibilities with the current setup.

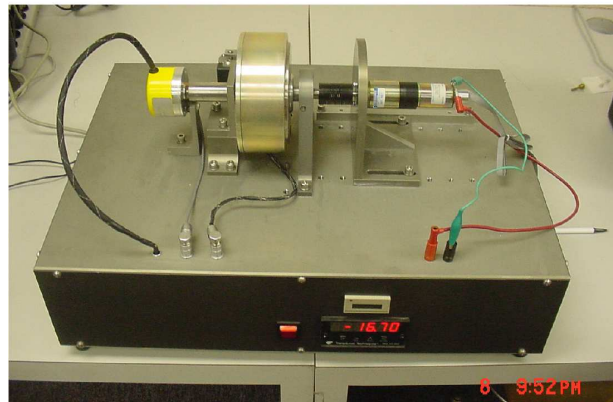


Fig. 1. The Fractional Horsepower Dynamometer developed at CSOIS.

## II. SYSTEM DESCRIPTION

### A. Architecture

The architecture of the dynamometer system is shown in Fig. 2. The Dynamometer includes the DC motor to be tested, a hysteresis brake for applying load to the motor, a load cell to provide force feedback, an optical encoder for position feedback and a tachometer for velocity feedback.

### B. Hardware Description

The Magtrol Hysteresis Brake used in the dynamometer produces torque strictly through an air gap, without the use of mag-

Corresponding author: Dr. YangQuan Chen. E-mail: yqchen@ece.usu.edu; Tel. (435)797-0148; Fax: (435)797-3054. URL: <http://www.csois.usu.edu/people/yqchen>.

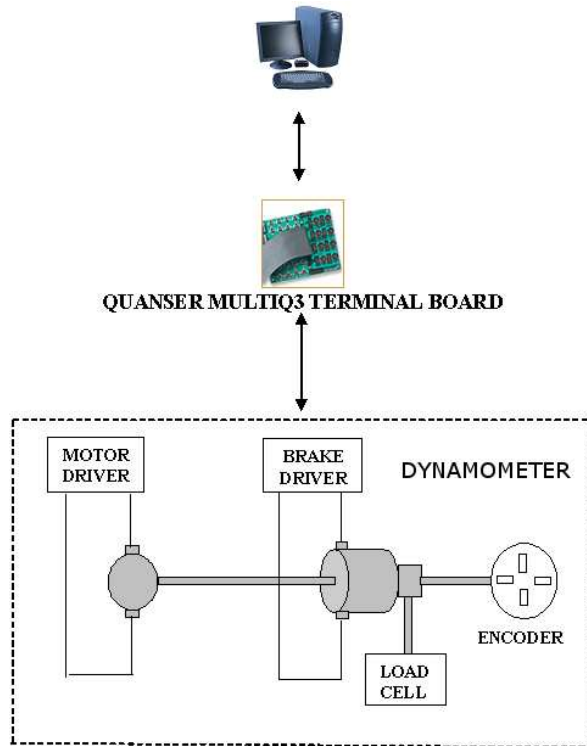


Fig. 2. The architecture of the fractional-horse power dynamometer control system.

netic particles or friction components. This method of breaking provides far superior characteristics (smoother torque, longer life, superior repeatability, higher degree of controllability, and less maintenance and down time) that makes it the preferred choice for precision tension control [11]. In this brake the control of torque is provided by a field coil. The amount of braking torque transmitted by the brake is proportional to the amount of current flowing through the field coil. The direction of current flow is of no consequence to the operation of brake. The brake and the motor are each driven by an Advanced Motion Controls Brush Type PWM Servo Amplifier Model 50A8. These controllers receive analog signals from data acquisition hardware. The PWM controllers use these signals to set the voltage output to the motor or the brake. The controller then supplies all the current needed to maintain the set voltage level.

Position and velocity measurements are performed on the dynamometer with the help of a Lucas Ledex S-9974-1024 incremental encoder. This encoder outputs 1024 bits per revolution on two quadrature lines. The system also has a Redington model no. 7631 tachometer for velocity measurement. This tachometer makes use of one of the quadrature signals supplied by the encoder to determine the velocity of the shaft.

The MDB-10 load cell from Transducer Techniques provides the force feedback on the dynamometer. The load cell senses torsional force from the hysteresis brake assembly. It consists of a flexing beam with a bonded strain gauge, producing an analog signal proportional to torque. With the heavy mass of the hysteresis brake, the load cell behaves somewhat like a spring. This can cause resonance at the system's natural frequency. To reduce such vibrations the moment arm of the brake is connected to a damper cylinder.

The data acquisition system for the dynamometer has two different sets of hardware for National Instruments (NI) LabVIEW

and Matlab/Simulink software platforms:

- The National Instruments 6021E series AT-MIO-16DE-10 is a 100 kS/s, 12-bit data acquisition card with 16 single-ended analog inputs. It has two 12-bit analog outputs, two 24-bit, 20 MHz counter/timers, and 32 digital I/O lines. The original hardware on the dynamometer has a 6021E terminal board that connects directly to the AT-MIO-16DE-10 card in the computer. NI LabVIEW based software uses this hardware to transmit control signals to the dynamometer.
- The dynamometer was modified to connect to a Quanser MultiQ3 terminal board in order to control the system through Matlab/Simulink Real-Time Workshop (RTW) based software. This terminal board communicates with the Quanser MultiQ3 data acquisition card and has 8 encoder inputs, 8 single-ended or differential analog inputs, 8 analog outputs, 16 digital inputs, and 16 digital outputs.

### C. Software Description

The dynamometer can be controlled from a personal computer using one of the following software platforms:

- The National Instruments LabVIEW software provides a graphical development environment for writing programs and developing graphical user interfaces (GUIs) to interface real world signals. The LabVIEW programs have been used to test various parameters like torque, current, speed, etc. for the DC motor. The GUI provides real-time parameter monitoring for the motor parameters.
- The complex nonlinear control schemes were tested using the Matlab/Simulink environment, which uses the WinCon application, from Quanser, to communicate with the Quanser MultiQ3 data acquisition card. WinCon is a Windows-based application that runs Simulink models in real-time on a PC. This brings rapid prototyping and hardware-in-the-loop simulation capabilities to Simulink models. The Matlab Real-Time Workshop generates C code from the Simulink model, which results in a Windows executable file that is run by WinCon independently of Simulink. WinCon's architecture ensures that the real-time process is afforded the highest CPU priority and is not preempted by any competing tasks other than the core OS functions.

## III. PROPOSED APPLICATIONS

### A. Research – Rapid Testing and Prototyping of Real-Time Non-linear Controllers

Without loss of generality, consider a servo control system modeled by:

$$\dot{x}(t) = v(t) \quad (1)$$

$$\dot{v}(t) = -f(t, x) + u(t), \quad (2)$$

where  $x$  is the position or displacement,  $f(t, x)$  is the unknown disturbance, which may be state-dependent or time-dependent,  $v$  is the velocity, and  $u$  is the control input. The system under consideration, i.e. the DC motor in the dynamometer, has a transfer function  $1.52/(1.01s + 1)$ . Moreover, the presence of the hysteresis brake allows us to add a time-dependent or state-dependent disturbance (load) to the motor. These factors combined can simulate a system similar to the one given by (1) and (2). A nonlinear controller can be designed for such a problem and can be tested in the presence of the real disturbance as introduced through the dynamometer. This eliminates the need for costly equipment to test nonlinear control algorithms and the system can be used as preliminary test bench for testing such theories. As shown in the next section, five nonlinear and adaptive control schemes, viz., adaptive feedforward cancelation (AFC), repetitive control

(RC), adaptive coulomb friction compensation (ACFC), state-periodic adaptive learning control (SPALC) for state-dependent disturbance, and sliding mode control (SMC) have been tested on the dynamometer as sample nonlinear control experiments.

**B. Education – Laboratory Experiments on Rapid Prototyping of Real-Time Controls**

The dynamometer testbed can be used as a part of laboratories in control and systems classes. In particular, at USU, two such applications are possible:

- 1) *Mechatronics Design Project Laboratory*: Since this is a course at the undergraduate level, the students can design simple PID controllers for the motor without considering any disturbance. Another exercise can be sensor calibration using the load-cell. The load-cell also has a display that displays the torque (in oz-in) being applied by the motor shaft on the load-cell. This system can also be used to teach the basics of hardware-software interfacing like the effect of sampling time on real-time simulation performance and how to deal with quantization effects in measured signals etc.
- 2) *Nonlinear and Adaptive Control*: The platform also provides an opportunity for experimentation in the Nonlinear and Adaptive Control class where students can design and test their controllers on the dynamometer.

**IV. SAMPLE NONLINEAR CONTROL EXPERIMENTS**

The test setup used for the experiments is shown in Fig. 3. Figure 4 shows the Simulink/RTW model used in one of the tests. Note that, Simulink/RTW automatically generates codes for Windows target to drive the dynamometer and brake via D/A blocks while the encoder block in Fig. 4 receives the shaft angular displacement information. Figure 4 is a typical hardware-in-the-loop real-time simulation.

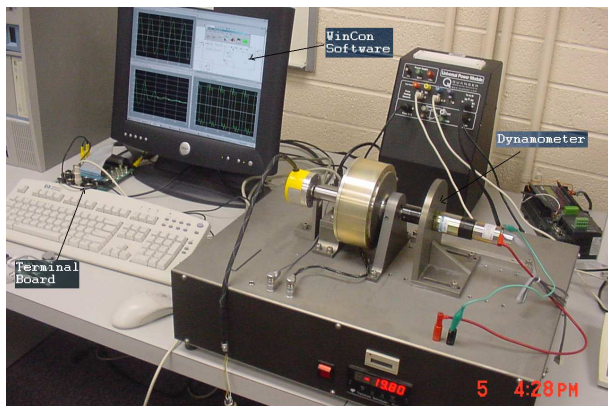


Fig. 3. The dynamometer setup used in the sample nonlinear control experiments.

**A. Adaptive Feedforward Cancellation (AFC)**

Tracking a reference signal and rejecting a time periodic disturbance has been a classical control problem. One of the techniques to reject time periodic disturbances is internal model principle in which a model of the disturbance generator is included in the control loop. This creates poles at the frequency of disturbance providing perfect disturbance rejection. Another approach is adaptive feedforward cancellation. In this method the disturbance is canceled at the input of the plant by adding a negative of its value at all times. Here magnitude and phase of the disturbance have to be estimated.

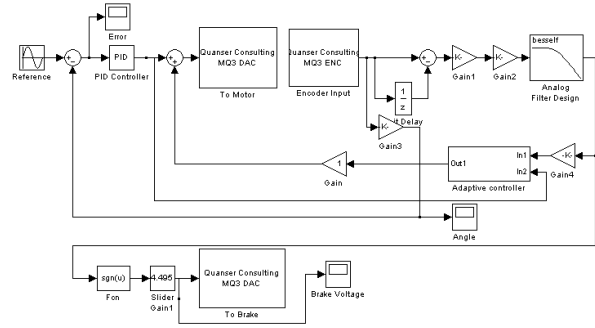


Fig. 4. Simulink/RTW model used in the sample nonlinear control experiments.

Let us consider an adaptive feedforward cancellation scheme as given in [4] for the plant described by (1) and (2). The plant is perturbed by a time-periodic disturbance  $d(t)$  of the form

$$d(t) = A \sin(\omega_1 t + \phi) = a_1 \cos(\omega_1 t) + b_1 \sin(\omega_1 t) \quad (3)$$

where only  $\omega$  is known. To compensate this kind of disturbance we need to modify the control law in the following way

$$u = u_1 + \theta_1 \cos(\omega_1 t) + \theta_2 \sin(\omega_1 t). \quad (4)$$

where  $u_1$  is the control law for the case without any disturbance; in our experiments it is a simple PID controller with gains  $K_p = 12$ ,  $K_i = 4$ , and  $K_d = 4$ . The control law in (4) cancels the disturbance exactly when the parameters  $\theta_1$  and  $\theta_2$  have the nominal values

$$\theta_1^* = -a_1, \quad \theta_2^* = -b_1. \quad (5)$$

The update law for ensuring the convergence of adaptive parameters can be written as [4]

$$\dot{\theta}_1 = -gy \cos(\omega_1 t), \quad \dot{\theta}_2 = -gy \sin(\omega_1 t) \quad (6)$$

where  $y$  is the plant output and  $g > 0$  is an arbitrary parameter called the adaptation gain.

Figure 5 shows the error plots for a velocity setpoint of 6 rad./sec. with a sinusoidal disturbance  $d(t) = 2.5 + 2 \sin(2t)$ . Note that in our experiments the control law does not directly cancel the brake voltage. Instead it controls the input to the motor depending upon the values of the adaptation parameters.

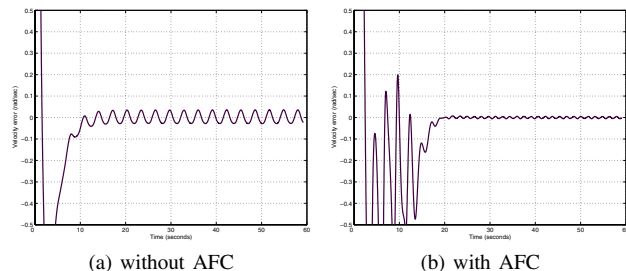


Fig. 5. Tracking error with and without the adaptive feedforward compensation

**B. Repetitive Control (RC)**

Another approach for effective tracking and disturbance rejection is by internal model principle using repetitive control ( see e.g. [5], [12], [13]). Repetitive control uses a delay of  $T$  seconds, which

is the period of the signal to be tracked or rejected, in the feedback path of an internal loop to create a transfer function  $(1)/(1-e^{-sT})$  inside the main control loop (Fig. 6). This causes the system to have infinite gain at the frequencies, which are multiples of the fundamental frequency, of the reference or the disturbance signal. A low-pass filter is also included to improve the stability and robustness. Note that this method can track signals of any shape provided their time period is known.

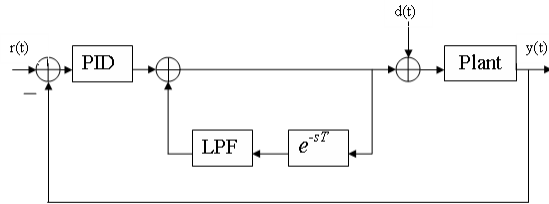


Fig. 6. Basic scheme for implementing continuous-time repetitive control.

We used  $r(t) = (2\pi)\sin((2\pi/20)t)$  as the reference signal and  $d(t) = 2.5 + 2\sin((2\pi/10)t)$  as the disturbance input. Fig. 7 shows the effect of repetitive control on the tracking error. The effect of the cut-off frequency  $\omega_c$  on the tracking error can also be seen in Figs. 7(b), 7(c), and 7(d).

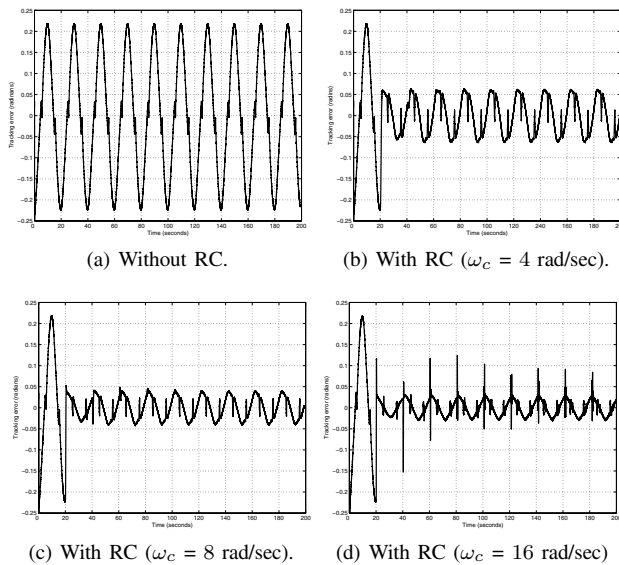


Fig. 7. Tracking error with and without Repetitive Control.

C. Adaptive Coulomb Friction Compensation (ACFC)

This section describes a method of adaptive friction compensation as given in [6]. This method estimates the friction by the use of a ‘reduced-order’ observer, the dynamics of which are designed to ensure asymptotic convergence of the estimation error to zero when the actual friction conforms to the classical model. If the actual model of the friction differs from the classical model, convergence of the error to zero cannot be easily shown; but the results show acceptable performance.

According to the classical definition friction is a nonlinear, zero-memory, odd-function of velocity. The simplest representation of this function is

$$f(v, a) = asgn(v) \tag{7}$$

where  $f$  is the friction force and  $v$  is the velocity. The dynamics of the velocity in the process in which friction is presented is assumed to be represented by

$$\dot{v}(t) = -f(v, a) + w \tag{8}$$

where  $w$  is the force due to all sources other than friction. In our case we can assume it to be the control voltage to the motor and friction can be introduced into the system by applying a voltage, proportional to the sign of velocity, to the brake.

In this method a nonlinear reduced-order observer has been postulated to estimate the undetermined parameter  $a$ . The observer is given by

$$\hat{a} = z - k|v|^\mu \tag{9}$$

where the gain  $k > 0$  and the exponent  $\mu > 0$  are design parameters and the variable  $z$  is given by

$$\dot{z} = k\mu|v|^{\mu-1}[w - f(v, \hat{a})]sgn(v). \tag{10}$$

Since real-world friction does not conform to the classical model, the performance of the observer in the presence of a more representative model

$$f(v) = a(2 + e^{-b|v|} + c|v|)sgn(v) \tag{11}$$

was investigated with  $a = 1.2$ ,  $b = 1.0$ , and  $c = 0.1$ .

Fig. 8 shows the position response of the dynamometer to a 0.05 Hz square wave with amplitude 2 radians in the presence of braking force governed by (11) with and without adaptive friction compensation.

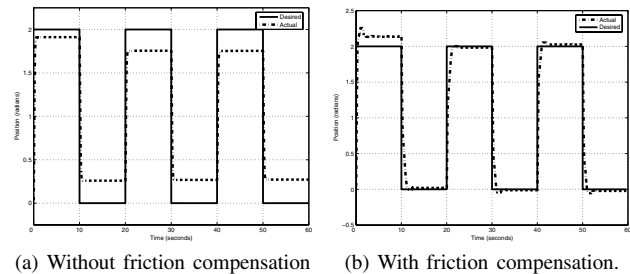


Fig. 8. Position response of system with and without friction compensation.

D. State-Periodic Adaptive Learning Control (SPALC)

This method, given in [7], presents a state-periodic adaptive learning control (SPALC) scheme for compensating a state-periodic disturbance. The system model used in this case is

$$\dot{x}(t) = v(t) \tag{12}$$

$$\dot{v}(t) = -a(x)sgn(v(t)) + u, \tag{13}$$

which is similar to the model from the previous case, the only difference being that here the disturbance depends on position (state).

To explain the idea of a state-periodic disturbance, we need some basic definitions. Let suppose that the system is trajectory-periodic like the upper figure of Fig. 9, where the forward and backward movements are repetitive. Then, there exist friction forces corresponding to the trajectory as in the bottom figure of Fig. 9. From this figure, since the trajectory is state-periodic (but not time-periodic), the following relationships are true:

$$x(t_a) = x(t_b) = x(t_c) = x(t_d),$$

$$t_b - t_a \neq t_d - t_c \text{ and } t_c - t_a \neq t_d - t_b$$

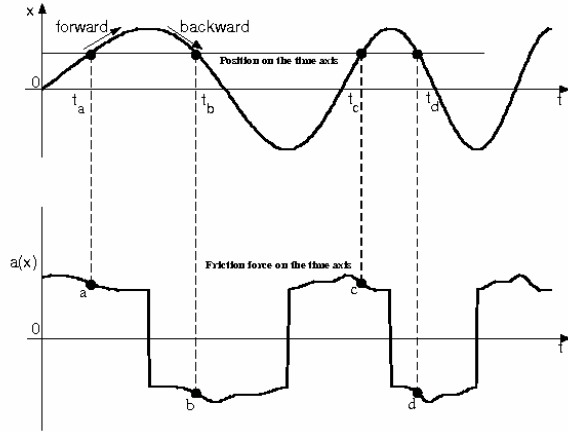


Fig. 9. The state-periodic trajectory and its corresponding state-dependent friction force.

In Fig. 9, the friction force values corresponding to time points  $t_a, t_b, t_c$  and  $t_d$  are represented by the points  $a, b, c$ , and  $d$ . Observe that  $a = c$  and  $b = d$ , because the friction force is position dependent. Now, based on Fig. 9, the following definitions are provided:

*Definition 4.1:* The total passed trajectory  $s$  is given as:

$$s = \int_0^t \frac{|dx(\tau)|}{d\tau} d\tau = \int_0^t |v(\tau)| d\tau,$$

where  $x(t)$  is the position, and  $v(t)$  is the velocity.

*Definition 4.2:* The periodic trajectory  $s_p$  is fixed and calculated, for example, by:

$$s_p = \int_{t_a}^{t_c} \frac{|dx(\tau)|}{d\tau} d\tau = \int_{t_b}^{t_d} \frac{|dx(\tau)|}{d\tau} d\tau$$

*Definition 4.3:* Since the friction force appears as a function of the position and the desired trajectory to be followed is assumed to be repetitive, which is true for many practical applications, the friction force is also periodic with respect to position. So, based on Definition 4.1 and Definition 4.2, the following relationship is true:

$$a(s) = a(s - s_p) \text{ and } x(s) = x(s - s_p) \quad (14)$$

*Definition 4.4:* The trajectory cycle ( $P_t$ ) at time instant  $t$  is defined as  $P$  that satisfies the following relationship:

$$\int_t^{t-P} \frac{|dx(\tau)|}{d\tau} d\tau = s_p$$

Particularly, the first trajectory cycle ( $P_1$ ) is defined as  $P$  such that:

$$\int_0^{t-P} \frac{|dx(\tau)|}{d\tau} d\tau = s_p$$

*Assumption 4.1:* The current position and time instant of the system are measured, and  $P_t$  can always be calculated at time instant  $t$ .

This assumption is true in the case of experiments with  $P_t$  being constantly updated using current position and time information.

With the above definitions and assumption, the following property is observed.

*Property 4.1:* The current friction force is equal to one-trajectory past friction force. That is,

$$a(t) = a(s(t)) = a(s(t) - s_p) = a(t - P_t) \quad (15)$$

The feedback control law used for this case, as given in [7], is given as

$$u = \hat{a}(t) \text{sgn}(v(t)) + \dot{v}_d(t) - (\alpha + \lambda)e_v(t) - \alpha \lambda e_x(t), \quad (16)$$

where  $\alpha$  and  $\lambda$  are positive gains,  $\dot{v}_d(t)$  is the desired acceleration, and  $e_x(t) = x(t) - x_d(t)$  is the position tracking error.

The periodic adaptation law for the case when  $s(t) \geq s_p$  is given by

$$\hat{a}(t) = \hat{a}(t - P_t) - K \text{sgn}(v(t)) (e_v(t) + \lambda e_x(t)) \quad (17)$$

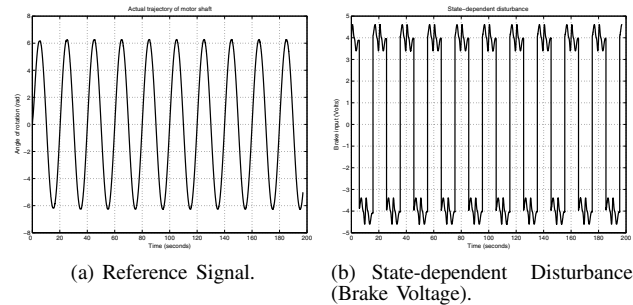
where  $\hat{a}(t - P_t) = \hat{a}(s - s_p)$  and  $K$  is a positive design parameter called the periodic adaptation gain.

The adaptation law when  $s(t) < s_p$  is given by

$$\hat{a}(t) = z - g(|v(t)|) \quad (18)$$

where  $\frac{1}{4} < g'(|v(t)|) < \infty$ ,  $\dot{z} = g'(|v|)[u - \hat{a} \text{sgn}(v)] \text{sgn}(v)$ , and  $g'(\cdot) = \frac{\partial g(\cdot)}{\partial \cdot}$ .

These control laws were verified on the dynamometer with sine wave reference of period 20 seconds. The reference trajectory and corresponding state-periodic disturbance are shown in Fig. 10.

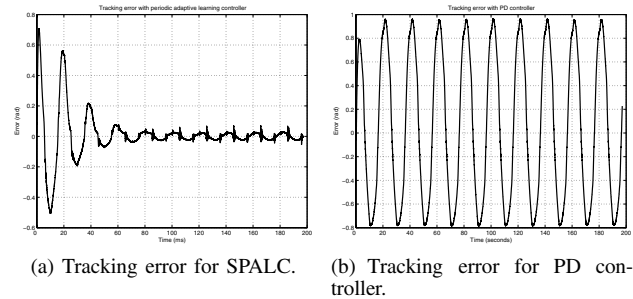


(a) Reference Signal.

(b) State-dependent Disturbance (Brake Voltage).

Fig. 10. Reference trajectory and state-periodic disturbance

Fig. 11 shows the asymptotic convergence of the tracking error to zero for the SPALC controller and compares it to a conventional PD controller.



(a) Tracking error for SPALC.

(b) Tracking error for PD controller.

Fig. 11. Reference trajectory and state-periodic disturbance

### E. Sliding Mode Control (SMC)

In sliding mode control, trajectories are forced to reach a sliding manifold in finite time and to stay on the manifold for all future time. Motion on the manifold is independent of matched uncertainties. For example, consider a second order system as given in [8]

$$\dot{x}_1 = x_2 \quad (19)$$

$$\dot{x}_2 = h(x) + g(x)u, \quad (20)$$

where  $h$  and  $g$  are unknown nonlinear functions and  $g(x) \geq g_0 > 0$  for all  $x$ . In order to stabilize the origin we design a control law that constrains the motion of the system to the manifold  $s = a_1 x_1 + x_2 = 0$ . On this manifold, the motion is governed by  $\dot{x}_1 = -a_1 x_1$ . Choosing  $a_1 > 0$  guarantees that  $x(t)$  tends to zero as  $t$  tends to infinity and the rate of convergence can be controlled by choice of  $a_1$ . Motion of the trajectory consists of a *reaching phase*, during which trajectories starting off the manifold  $s = 0$  move toward it and reach it in a finite time, followed by a *sliding phase*, during which the motion is confined to the manifold  $s = 0$  and the dynamics of the system are represented by the reduced-order model  $\dot{x}_1 = -a_1 x_1$ .

Now let us consider the sliding mode control of a pendulum equation, as given in [8],

$$\dot{x}_1 = x_2 \quad (21)$$

$$\dot{x}_2 = -(g_0/l) \sin(x_1 + \delta_1) - k_0/m + (1/ml^2)u \quad (22)$$

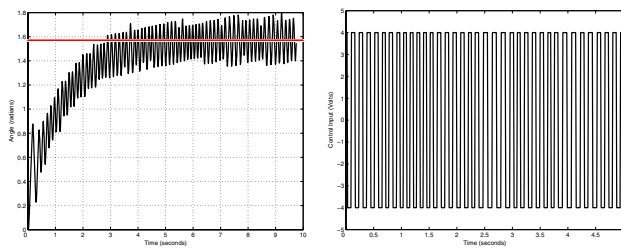
$$u = -k \operatorname{sgn}(s) = -k \operatorname{sgn}(a_1 x_1 + x_2) \quad (23)$$

to stabilize the pendulum at  $\delta_1 = \pi/2$ , where  $x_1 = \theta - \delta_1$  and  $x_2 = \dot{\theta}$ . The constants  $m$ ,  $l$ ,  $k_0$ , and  $g_0$  are the mass, length, coefficient of friction, and acceleration due to gravity, respectively. We take  $a_1 = 1$  and  $k = 4$ . An emulation of this system can be implemented by the dynamometer/DC motor setup described in the paper.

Fig. 12 shows the step response of the DC motor with the control law given by (23). This phenomenon is called *chattering* and occurs because of imperfect switching due to unmodeled system dynamics. To eliminate the chattering, the control input is divided into continuous and switching components so as to reduce the amplitude of the switching component. This results in a control law

$$u = -0.1x_2 + 2\cos x_1 - 2\operatorname{sgn}(s) \quad (24)$$

which shows a reduction in the switching term amplitude from 4 to 2. Fig. 13 shows the elimination of chattering in step response and control input. Note that the parameters in the control law, as well as the system parameters, have been modified from [8] in order to satisfy the voltage constraints of the dynamometer hardware.

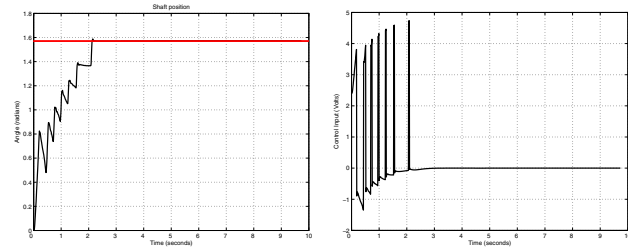


(a) Step response for  $\pi/2$  radians. (b) Control input to the motor.

Fig. 12. Step response and control input for sliding mode controller.

## V. CONCLUSION

This paper demonstrates the use of a dynamometer system as a low-cost and self-contained platform to test nonlinear control algorithms. Five proven nonlinear control schemes have been demonstrated on the dynamometer with experimental results shown in Sec. IV. It should be noted here that the total load on the motor shaft includes mechanical friction in the moving part and load due to imperfect linkages etc., apart from just braking force. Moreover, some of the parameters of the system to be simulated have to be modified in order to meet system constraints. Thus ideal results cannot be achieved in practical conditions. But still, the



(a) Step response for  $\pi/2$  radians. (b) Control input to the motor.

Fig. 13. Step response and control input for the modified sliding mode controller.

experimental results are comparable to the results of pure software simulations.

Future work on this platform can include the simulation of other nonlinear systems such as the hydraulic servo-system. Also, other nonlinear control schemes, such as backstepping and feedback linearization etc. [2], remain to be tested on the platform. We also scheduled to add relevant lab components in our curricula for classroom trial use of this general purpose platform.

## ACKNOWLEDGEMENT

We would like to thank the financial support from CSOIS for building the original fractional horsepower dynamometer as a senior design project under the supervision of Dr. Carl Wood.

## REFERENCES

- [1] P. V. Kokotovic, "1991 Bode lecture - the joy of feedback: Nonlinear and adaptive," *IEEE Control Systems Magazine*, vol. 1992, no. 6, pp. 7-17, June 1992.
- [2] P. V. Kokotovic and M. Arcak, "Constructive nonlinear control: Progress in the 90s," in *Proc. of the 14th IFAC World Congress*, Beijing, China: IFAC, 1999, pp. 49-77.
- [3] M. Mecham, M. Johnson, L. Mecham, E. Flygare, and S. Anderson, "Fractional horse-power dynamometer," 2000, senior Project Report, Dept. of Electrical and Computer Engineering, Utah State University.
- [4] M. Bodson, A. Sacks, and P. Khosla, "Harmonic generation in adaptive feedforward cancellation schemes," *IEEE Trans. on Automatic Control*, vol. 39, no. 9, pp. 1939-1944, 1994.
- [5] Y. Q. Chen, M. Ding, L. Xiu, K. Ooi, and L. Tan, "Optimally designed parsimonious repetitive learning compensator for hard disc drives having high track density," *US Patent*, no. 6,574,067, June 2003.
- [6] B. Friedland and Y.-J. Park, "On adaptive friction compensation," *IEEE Trans. on Automatic Control*, vol. 37, no. 10, pp. 1609-1612, 1992.
- [7] Hyosung Ahn and YangQuan Chen and Yashodhan Tarte, "State-dependent friction force compensation using periodic adaptive learning control," *IFAC Control Engineering Practice*, p. (revised), 2006.
- [8] H. K. Khalil, *Nonlinear Systems*, 3rd ed. Upper Saddle River, NJ: Prentice Hall, 2002.
- [9] W. Ren, "ECE7330 Nonlinear and Adaptive Control," <http://www.engineering.usu.edu/classes/ece/7330>, Spring 2006.
- [10] YangQuan Chen, "ECE5320 Mechatronics," <http://mechatronics.ece.usu.edu/>, Spring 2006.
- [11] Magtrol, "Magtrol hysteresis brakes," <http://www.magtrol.com/brochures/hysteresis.pdf>.
- [12] Chen, YangQuan, "Parsimonious ILC and RC: Seagate Experience," *Iterative Learning Control International Summer School at Utah State University*, vol. [Online Slides] [http://www.csois.usu.edu/ilc/summerschool03/ILC\\_ISS\\_03\\_Chen.pdf](http://www.csois.usu.edu/ilc/summerschool03/ILC_ISS_03_Chen.pdf), pp. 1-199, June 2003.
- [13] R. Costa-Castelló, J. Nebot, and R. Grinó, "Demonstration of the internal model principle by digital repetitive control of an educational laboratory plant," *IEEE Transactions on Education*, vol. 48, no. 1, pp. 73-80, February 2005.